Supporting Information

Nyberg et al. 10.1073/pnas.1012651108

SI Methods

Structural MRI Analyses. The supervised voxel-based morphometry protocol proceeded in the following stages for the longitudinal analysis:

(*i*) T1-weighted images were segmented using a segmentation algorithm (modified version of unified segmentation) developed in SPM8 to produce GM and WM images in the native space of the T1-weighted MRI scans. This algorithm is essentially the same as the one described by Ashburner and Friston (1) but includes unique tissue probability maps (e.g., bone, soft tissue, air) that lead to more robust initial affine registration and better modeling of different tissues. The remaining procedure stream used the DARTEL toolbox (2).

(*ii*) Tissue class images (e.g., GM, WM) were rigidly aligned (with the tissue probability map) using the normalization parameter exploited from the segmentation step and resampled to isotropic voxels (1.5 × 1.5 × 1.5 mm).

(*iii*) A subject-specific template was created using a registration algorithm that involved the simultaneous registration of GM/WM from time point 1 (2002) to GM/WM from time point 2 (2008), respectively. The procedure of creating a template was an iterative procedure that began by producing an initial template as a mean of within-subject GM/WM across the two sessions (2002 and 2008). Deformations from the initial template to each of the GM/WM images were computed, and the inverse of deformation was applied to each of the GM/WM images. A second template was created as the mean of the deformed GM/WM images across the two sessions, and this procedure was repeated until convergent criteria was reached.

(*iv*) A group-specific template was created from all subject-specific templates (37 subjects). The procedure to create a group-specific template was generally the same as that for the subject-specific template but involved additional spatial smoothing to achieve better alignment between subjects.

(*v*) The flow field computed for each subject in step *iv*, warping rigidly aligned GM/WM to the common DARTEL space, was composed with an affine transformation that transforms DARTEL to MNI space. To account for potential contraction and expansion induced by warping, the final normalized warped GM and WM images were scaled by Jacobian determinants (modulation).

(*vi*) The final images, which were subject-specific GM and WM volume maps for each participant, were smoothed with an 8-mm full-width at half-maximum Gaussian kernel (final voxel size: 2 × 2 × 2 mm). For the cross-sectional analysis, the procedure was generally the same as the one described above but excluded subject-specific template creation.

Fusion ICA. Joint ICA is a multivariate technique to analyze two different data types jointly by assuming a common linear mixture between two modalities. Such an approach allows for investigation of the relationship between all voxels in both modalities in the sense that variation in one modality is attributed to the other in a linear context. A full description of fusion ICA is given by Calhoun et al. (3). In short, fusion ICA proceeded in the following steps:

(*i*) As an initial feature selection step, a statistical parametric mapping contrast image for categorization and a (smooth normalized) GM segmentation image were set up per time point for each individual.

(*ii*) Normalization was conducted on both features to produce the same average sum-of-squares. This step compensated for different ranges associated with each modality by producing a similar unit, in which within-modality scaling is preserved.

(*iii*) The two modalities were composed in a data matrix in a way that each row and column stand for a subject and a voxel, respectively.

(*iv*) Principal component analysis was conducted to reduce dimensionality of the composed matrix to the one estimated by minimum description length criteria (4).

(*v*) Finally, maximally independent components as well as subject-specific loading parameters (loading parameters reflect how strongly each subject contributes to a specific component) were extracted using the Infomax algorithm (5). A component was further analyzed if and only if its corresponding loading parameters showed a significant difference (using a paired *t* test) between two time points.

SI Results

Structural–Functional MRI Fusion. The fMRI feature of the significant component reflected functional decline in the bilateral cerebellum, left precuneus, left anterior cingulum, left inferior frontal, and left hippocampus regions as well as in the bilateral inferior occipital and right middle frontal regions. The GM feature of the component showed GM loss in the bilateral cerebellum, middle occipital, left precuneus, left inferior frontal, left caudate, right middle temporal, and right inferior parietal regions as well as in the right middle frontal regions (Table S7). The premise was that GM reductions for regions in the structural feature were associated with regions showing functional decline in the fMRI feature, suggesting that GM changes were related to functional changes either locally or distally. Critically, age-related frontal atrophy locally accounted for the diminished frontal responses (i.e., there was an overlap between structural and functional features of the component in the frontal region), whereas there was no overlap in structural and functional features for the occipital region, indicating that functional changes were induced by distal structural changes.

1. Ashburner J, Friston KJ (2005) Unified segmentation. *NeuroImage* 26:839–851.
2. Ashburner J (2007) A fast diffeomorphic image registration algorithm. *NeuroImage* 38: 95–113.
3. Calhoun VD, et al. (2006) Method for multimodal analysis of independent source differences in schizophrenia: Combining gray matter structural and auditory oddball functional data. *Hum Brain Mapp* 27:47–62.
4. Calhoun VD, Adali T, Pearlson GD, Pekar JJ (2001) A method for making group inferences from functional MRI data using independent component analysis. *Hum Brain Mapp* 14:140–151.
5. Bell AJ, Sejnowski TJ (1995) An information-maximization approach to blind separation and blind deconvolution. *Neural Comput* 7:1129–1159.

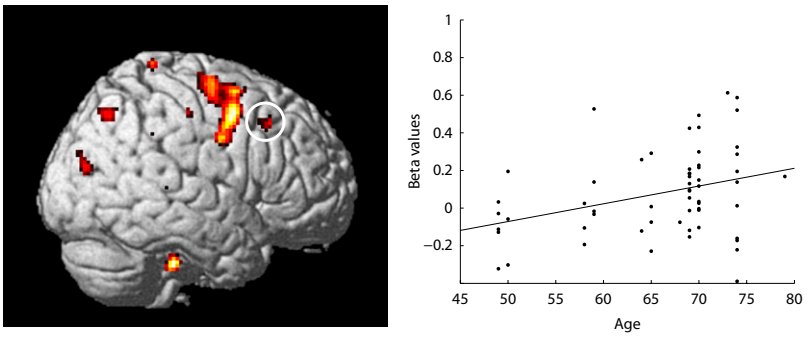

Fig. S1. A cross-sectional analysis of brain activity across all 60 participants from time point 1 showed significant positive correlations with age in several brain regions, including the frontal cortex. (*Left*) Rendering is thresholded at $P < 0.005$ for illustrative purposes. (*Right*) Activity in circled region on the rendering is plotted as a function of age, showing a significant positive correlation ($r = 0.34$, $P = 0.009$).

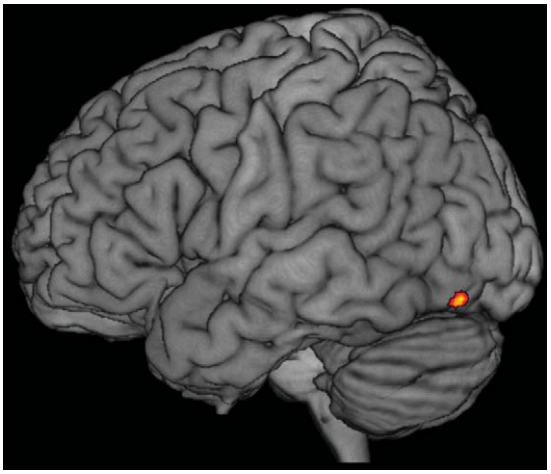

Fig. S2. Reduced brain activity as a function of age in the occipital cortex. The occipital reduction was significant for cross-sectional analysis of fMRI data from the 2002 session ($x, y, z = -34, -56, -16$; $t = 3.39$). The statistical threshold set to $P < 0.005$ is uncorrected for illustrative purposes.

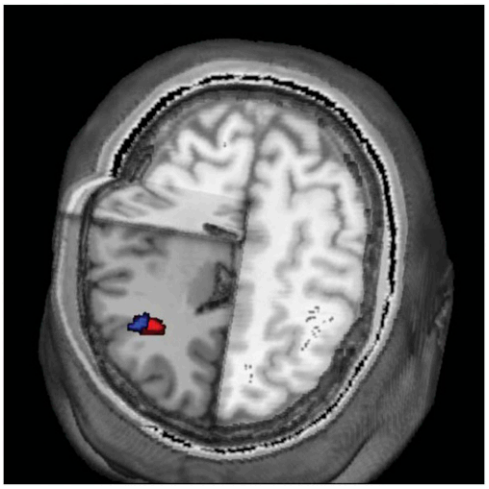

Fig. S3. Longitudinal structure–function relation in the right frontal cortex. There is a clear overlap in the right frontal cortex indicating that the decreased brain activity level as a function of age can be explained, to some extent, in terms of GM atrophy (red, functional decline; blue: atrophy).

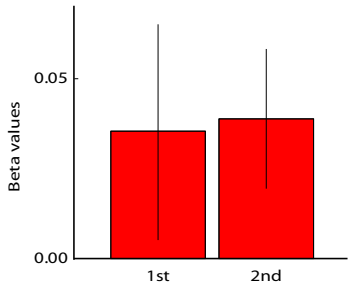

Fig. S4. Assessment of practice effects on right frontal cortex activity (peak coordinate as in Fig. 3). From the pool of participants, individuals were selected to allow a comparison of right frontal activity when age was held constant across sessions (74 ± 2 y) and the categorization task was performed for the first (first bar, $n = 12$) or second (second bar, $n = 15$) time. Thus, we zoomed in on the age range of 65–75 y, wherein we had the most participants, and compared those subjects in this age range during their first fMRI session with individuals 5 y younger who were about the same age at their second fMRI session. No evidence for a practice effect was observed. Bars indicate SEM.

Table S1. Longitudinal GM loss across the whole brain

Region	*x, y, z*	*t* value	Cluster size
R-Thalamus	8, −18, 10	8.16	180
L-Postcentral	−42, −10, 50	7.16	65
L-Angular	−46, −62, 32	6.32	70
L-Cerebellum	−20, −80, −42	6.26	124
L-Thalamus	−6, −6, 14	6.05	52
R-Postcentral	52, −2, 34	5.35	35
R-Cerebellum	18, −78, −30	5.96	126
L-Caudate	−12, 14, 12	5.53	47
L-Midtemporal	−52, −34, 4	5.32	62
R-Inferior frontal	30, 28, −8	5.18	21

$P < 0.005$ false discovery rate, cluster-level $P < 0.05$ FWE.

Table S2. Cross-sectional (2002 and 2008) GM loss with increasing age

Region	*x, y, z*	*t* value	Cluster size
2008			
L-Midtemporal	−56, −30, −6	5.32	997
R-Midtemporal	54, −12, −16	4.05	1,308
R-Cerebellum	20, −72, −54	4.03	613
L-Cerebellum	−18, −78, −50	4.01	922
L-Midoccipital	−20, −82, 20	4.00	22
L-Fusiform	−36, −76, −12	4.00	48
L-Inferior frontal	−40, 6, 26	3.86	129
R-Putamen	22, 10, −6	3.59	150
R-Superior marginal	54, −44, 28	3.58	97
R-Cerebellum	32, −66, −22	3.49	236
L-Cerebellum	−30, −66, −26	3.46	177
R-Inferior frontal	42, 10, 30	2.97	21
L-Postcentral	−48, −10, 32	2.86	17
L-Putamen	−20, 8, −8	2.86	13
2002			
R-Inferior temporal	54, −24, −22	4.23	207
L-Inferior frontal	−40, 26, 8	3.33	50
R-Inferior frontal	50, 10, 6	3.16	31
R-Superior occipital	24, −72, 24	2.92	10
L-Midtemporal	−58, −28, −8	2.86	12
R-Cerebellum	28, −68, −22	2.86	25
L-Inferior frontal	−40, 10, 30	2.84	12

$P < 0.001$ uncorrected, $k > 10$.

Table S3. Longitudinal WM matter loss

Region	*x, y, z*	*t* value	Cluster size
Corpus callosum	−6, −22, 20	8.29	11,782
L-Precuneus WM	−12, −46, 14	6.72	Subregion
L-Parahippocampal WM	−28, −40, −2	5.87	Subregion
R-Hippocampal WM	36, −8, −14	5.48	Subregion
R -Putamen WM	24, 16, 10	5.47	Subregion
R-Precuneus WM	18, −42, 2	4.35	Subregion
R-Anterior cingulum WM	14, 36, 8	3.91	Subregion
R-Parahippocampal WM	20, −34, −8	3.41	Subregion
L-Temporal WM	−38, 4, −28	5.89	468
L-Frontal WM	−28, 54, −14	4.76	209
R-Orbitofrontal WM	26, 54, −8	4.55	365
R-Motor white matter	10, 20, 54	4.25	76
L-Precuneus WM	−8, −44, 56	4.01	21

$P < 0.05$ false discovery rate, $k > 20$.

Table S4. Activity increases during the categorization task (2002 and 2008)

Region	*x, y, z*	*t* value	Cluster size
2008			
L-Fusiform	−44, −64, −16	17.93	41,519
L-Cerebellum	−40, −52, −28	17.48	Subregion
R-Lingual	20, −88, −12	16.92	Subregion
R-Cerebellum	30, −50, −30	16.79	Subregion
L-Inferior occipital	−34, −92, −8	15.44	Subregion
L- Supplementary motor	−4, −4, 62	15.26	Subregion
L-Inferior frontal	−40, 4, 30	13.49	Subregion
R-Midoccipital	32, −90, 8	13.42	Subregion
L-Midoccipital	−26, −96, 8	13.35	Subregion
L-Inferior parietal	−46, −36, 48	13.24	Subregion
L-Precentral	−48, −4, 48	13.02	Subregion
L-Inferior temporal	−52, −48, −18	12.35	Subregion
R-Fusiform	32, −66, −10	10.31	Subregion
L-Putamen	−30, 10, −2	9.71	Subregion
L-Inferior frontal	−46, 36, 0	8.75	Subregion
R-Midfrontal	38, −4, 60	8.64	Subregion
L-Midtemporal	−56, −50, 2	8.43	Subregion
L-Inferior frontal	−38, 28, −14	8.17	Subregion
R-Insula	32, 22, −2	10.03	631
R-Superior occipital	30, −66, 40	9.09	737
R-Supramarginal	40, −30, 36	7.32	165
2002			
L-Inferior occipital	−34, −90, −10	16.02	9,306
L-Cerebellum	−44, −60, −22	15.95	Subregion
R-Midoccipital	30, −92, 8	13.94	Subregion
L-Inferior occipital	−44, −68, −14	13.48	Subregion
R-Cerebellum	28, −44, −28	13.03	Subregion
L-Fusiform	−32, −78, −16	9.94	Subregion
L-Supplementary motor	−2, −4, 56	12.31	900
L-Precentral	−40, −10, 60	12.08	6,077
L-Midfrontal	−26, −10, 52	11.90	Subregion
L-Inferior parietal	−44, −38, 42	11.33	Subregion
L-Inferior frontal	−48, 10, 28	9.03	Subregion
L-Hippocampus	−26, −28, −4	10.03	2,335
R-Putamen	24, 6, 10	8.66	410
R-Inferior frontal	36, 26, −6	8.26	100
R-Precentral	38, −6, 56	8.23	714
R-Superior temporal	54, 18, −8	8.20	66
L-Superior temporal	−52, 16, −8	7.92	87
L-Caudate	−16, 28, 2	7.50	20
L-Putamen	−24, 12, 6	7.44	31
L-Midtemporal	−54, −52, 2	6.59	24
R-Inferior parietal	46, −48, 44	6.45	37
L-Inferior frontal	−34, 24, −8	6.36	31

$P < 0.05$ FWE, $k > 20$.

Table S5. Longitudinal functional increase (i.e., greater activation at follow-up)

Region	*x, y, z*	*t* value	Cluster size
L-Parahippocampus	−20, −6, −28	4.50	35
L-Midtemporal	−32, 16, −38	4.38	36
L-Superior motor	−8, −2, 70	4.33	28
R-Midoccipital	48, −78, 20	4.27	21
L-Operculum Rolandic	−58, −6, 10	4.16	14
R-Superior temporal	64, −28, 6	4.10	21
L-Superior occipital	−16, −92, 16	3.95	80

$P < 0.001$ uncorrected, $k > 10$.

Table S6. Behavioral performance

		Longitudinal result			Baseline results		
Task	*n*	T1	T2	*P**	Remainders	Dropouts	$P^{\dagger}$
Episodic memory performance[‡]	36	21.0 (5.6)	19.9 (6.0)	0.11	20.2 (5.5)	17.6 (3.8)	0.05
Semantic memory performance[§]	37	24.6 (3.4)	23.6 (3.6)	0.05	24.0 (4.4)	23.1 (3.6)	NS
fMRI performance							
Word categorization accuracy[¶]	38	152.8 (12.8)	156.3 (7.5)	0.01	151.9 (14.2)	154.6 (5.9)	NS
Word categorization mean RT	38	1071 (163)	106.1 (151)	NS	1097 (167)	1146 (118)	NS
Postscan recognition test[‖]	35	105.5 (17.7)	102.1 (15.6)	0.06	104.6 (19.7)	87.5 (18.8)	0.004

*Paired-sample *t* test (one-tailed), [†]Student's *t* test (one-tailed), and [‡]composite score (maximum = 42) are based on three tests: face recognition, verbal recall, and recall of actions; a detailed description of these tests is provided by Ashburner and Friston (1).
§Word comprehension (maximum = 30), [¶]maximum = 160, and [‖]hits minus false alarms (maximum = 160) are based on 27 subjects.

1. Ashburner J, Friston KJ (2005) Unified segmentation. *NeuroImage* 26:839–851.

Table S7. MNI coordinates for fMRI and GM MRI features of the significant component (positive direction)

Region	*x, y, z*	*Z* value	Cluster size
fMRI feature			
L-Lingual	14, −96, −6	13.94	6,870
L-Inferior occipital	−12, −94, −8	13.50	Subregion
L-Cerebellum	−32, −80, −20	11.98	Subregion
R-Cerebellum	22, −84, −22	8.80	Subregion
R-Inferior occipital	32, −92, −8	6.99	Subregion
L-Precuneus	0, −66, 60	6.39	293
L-Anterior cingulum	−4, 22, 30	4.41	323
L-Inferior frontal	−52, 20, 34	3.81	29
R-Midfrontal	50, 26, 38	3.55	30
R-Midfrontal	**34, 38, 36**	**3.55**	**49**
L-Hippocampus	−20, −26, −10	3.52	15
MRI feature			
R-Cerebellum	14, −84, −34	8.79	9,211
L-Cerebellum	−14, −72, −46	8.17	Subregion
L-Cerebellum	−40, −58, −50	5.13	Subregion
R-Inferior parietal	46, −40, 56	8.37	1,642
L-Precuneus	−12, −70, 38	6.86	2,896
L-Postcentral	−48, −18, 34	6.69	Subregion
L-Angular	−44, −62, 36	4.90	Subregion
L-Inferior frontal	−46, 28, 4	5.70	90
R-Midfrontal	34, 6, 36	5.60	202
L-Midoccipital	−34, −84, 4	5.25	168
R-Midtemporal	44, −58, 0	4.67	69
R-Superior temporal	56, −32, 14	4.38	148
R-Cuneus	18, −62, 38	4.30	92
R-Superior frontal	18, 5, 52	4.28	57
L-Mid-Frontal	−24, 28, 56	4.28	52
R-Midfrontal	32, 52, 22	4.20	216
L-Midcingulum	0, 28, 36	3.79	57
R-Superior occipital	28, −74, 18	3.58	35
L-Caudate	−12, 18, 8	3.53	28
R-Midfrontal	30, 22, 56	3.52	15
R-Midfrontal	**40, 38, 38**	**3.51**	**17**

Overlapping right frontal region is shown in bold. $Z > 3.5$, $k > 10$.